

## Relevance of surface reconstruction to specular RHEED intensity on GaAs(001)

Makoto Itoh\* and Takahisa Ohno

National Research Institute for Metals, 1-2-1, Sengen, Tsukuba, Ibaraki 305-0047, Japan

(Received 29 November 1999; revised manuscript received 14 February 2000)

By carrying out atomic-scale growth simulations of a GaAs(001)- $\beta 2(2 \times 4)$  surface, we find that the density of double As dimers evolves synchronously with the observed specular reflection high-energy electron-diffraction (RHEED) intensities in growth and after its interruption. At the same time, we find that a step density does not even oscillate during growth. We further show that the structural transition of initial growing islands from a non- $(2 \times 4)$  structure to the  $\beta 2(2 \times 4)$  structure found previously can be detected *in situ* by specular RHEED observation. The fast and slow recovery processes after growth interruption are identified, respectively, as the incorporation of Ga adatoms to surface structures, and the phase ordering of various domains consisting of the  $\beta 2(2 \times 4)$  structure. We also relate these results to a specular RHEED intensity with the help of *ab initio* calculations.

### I. INTRODUCTION

Thin-film growth on a GaAs(001) surface, either homoepitaxial or heteroepitaxial, has a great technological importance when developing optoelectronic devices. To monitor the growth of such a film and to evaluate its quality, molecular-beam epitaxy (MBE) and reflection high-energy electron diffraction (RHEED) are often used in combination.<sup>1</sup> In particular, since the discovery of a specular RHEED intensity oscillation,<sup>2-4</sup> this phenomenon was extensively used to monitor growth and to estimate a growth rate as a function of a cation flux.<sup>5-7</sup>

In this study, we investigate the homoepitaxial growth of a GaAs(001) surface, on which it is known that there are four different kinds of  $2 \times 4$  structures:  $\alpha(2 \times 4)$ ,  $\beta 1(2 \times 4)$ ,  $\beta 2(2 \times 4)$ , and  $\gamma(2 \times 4)$  structures.<sup>8</sup> After several years' debate, the  $\beta 2(2 \times 4)$  structure was confirmed to be the most stable structure on GaAs(001), while other metastable structures are found to appear depending on the growth conditions used.<sup>8-10</sup> Among the four  $2 \times 4$  structures, the most stable  $\beta 2(2 \times 4)$  structure and the metastable  $\beta 1(2 \times 4)$  structure are depicted in Figs. 1(a) and 1(b), respectively.

On the origin of a specular RHEED intensity oscillation, conversely, there are still several controversial arguments.<sup>11</sup> Among them, one of the appealing ideas is that the time evolution of a step density gives rise to this oscillation.<sup>5</sup> To try to support this interpretation of the experimental results,<sup>5</sup> many theoretical as well as experimental investigations have been carried out. For instance, comparisons were made between the specular RHEED intensity oscillations observed during growth of Si(001) or GaAs(001) and the calculated step densities by kinetic Monte Carlo (MC) simulations with the use of the one-species solid-on-solid (SOS) model.<sup>12-14</sup> Furthermore, by using scanning tunneling microscopy (STM), Sudijono and co-workers directly counted the "step densities" after interrupting growth of the (001) and (111)A surfaces of GaAs at several different deposition coverages, followed by quenching them down to room temperature.<sup>15-17</sup> In these experimental studies, quite a good agreement was obtained by using samples on which growth was interrupted when the surfaces were in the steady-state growth mode at

high temperatures. However, the definition of a step density used in the kinetic MC calculations<sup>12-14</sup> and the counting in the STM images<sup>15-17</sup> is actually not the density of steps but that of terrace edges. For clarity, let us denote the densities of atomic steps and terrace edges by  $\rho_s$  and  $\rho_e$ , respectively. Between them, the conventional definition of a "step density" obviously corresponds to  $\rho_e$ , for which the approximate relation  $\rho_e \approx \rho_s$  holds on Si(001).<sup>18,19</sup> However, since an atomically flat polar semiconductor surface is unstable, this relation no longer holds on GaAs(001) or GaAs(111)A.<sup>15-17</sup> Instead, the relation  $\rho_s \gg \rho_e$  actually holds

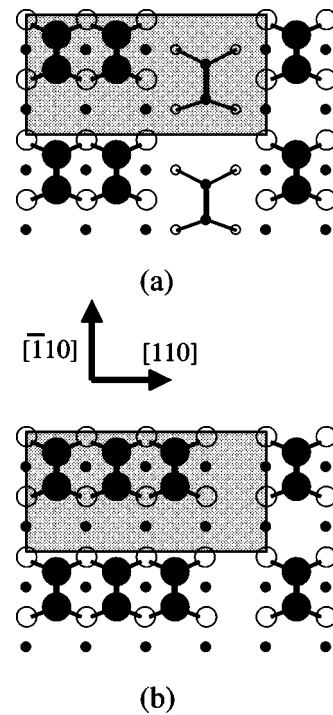


FIG. 1. Plan views of (a) the  $\beta 2(2 \times 4)$  structure and (b) the  $\beta 1(2 \times 4)$  structure. The unit cells and the crystallographic directions are indicated by the shaded rectangles and the arrows, respectively. The dark and bright disks denote As and Ga atoms, respectively, and their radii decrease according to their depths.

on them. Therefore, if we denote a specular RHEED intensity by  $I_s$ , the relation that Sudijono and co-workers found is not represented by  $\Delta I_s \propto -\Delta \rho_s$  but by  $\Delta I_s \propto -\Delta \rho_e$ , where  $\Delta I_s$  indicates the time evolution of  $I_s$ , and so on. Here again,  $\Delta \rho_s \neq \Delta \rho_e$  in general. More importantly, the relation  $\Delta I_s \propto -\Delta \rho_e$  does not imply any causal relations between  $I_s$  and  $-\rho_e$ . Instead, it merely implies the existence of a positive correlation between them.

In a conventional kinetic MC simulation of surface growth on GaAs(001), the one-species SOS model on the simple cubic lattice was used,<sup>13,14</sup> with the combined use of a step density, which is actually neither  $\rho_s$  nor  $\rho_e$ . This is because this model has no true atomic scale structures and, hence, no snapshots generated with the use of it correspond to any real atomic structures on GaAs(001). Therefore, it indeed remains unclear if a step density is relevant to the time evolution of  $I_s$ . To examine this, we estimate the length scales of several physically relevant quantities used in the conventional explanations.<sup>6,13,14</sup> Let us first denote the de Broglie wavelength of an incident electron beam used in RHEED observation by  $\lambda$  and an incident energy by  $E$ . Then, since  $E$  is larger than 10 keV,  $\lambda < 0.13 \text{ \AA}$ , which is shorter than the surface lattice constant  $a_s = 4.0 \text{ \AA}$  or a bilayer height  $h_{bulk} = 2.8 \text{ \AA}$  of a bulk GaAs(001). This means that a surface atomic structure, symbolically denoted by  $f(\mathbf{x})$  as a function of atomic coordinates  $\mathbf{x}$ , is sufficiently smooth when observed by using RHEED. Accordingly, a change of a surface structure by atomic-scale kinetics, such as growth, is regarded as the local deformation of  $f(\mathbf{x})$  to  $f(\mathbf{x}) + \delta f(\mathbf{x})$ . By this change, the Fourier transform  $F(\mathbf{q})$  of  $f(\mathbf{x})$ , with  $\mathbf{q}$  a momentum transfer between incident and diffracted electron beams, is influenced, though in general there may be a  $\mathbf{q}$  dependence in the sensitivity of  $F(\mathbf{q})$ . Accordingly, the fact that fractional and other RHEED spot intensities have been used to determine surface structures<sup>20–22</sup> means that a specular RHEED intensity must also reflect a change of  $f(\mathbf{x})$  denoting a surface atomic structure. In other words, to claim that only a specular intensity depends upon a step density is equivalent to claiming that a singularity exists in  $f(\mathbf{x})$  associated with the presence of an atomic step. As we saw before, however, this is not the case when  $E > 10 \text{ keV}$ . Therefore, a step density and a specular RHEED intensity have no causal relations to each other, and, hence, it is incorrect to attribute the microscopic origin of a specular RHEED intensity oscillation to the time evolution of a step density.<sup>12–17</sup> Incidentally, in the specular condition, a momentum transfer  $\mathbf{q}$  reduces to  $\mathbf{q} = |\mathbf{q}| \mathbf{n}_\perp$ , where  $\mathbf{n}_\perp$  denotes a unit vector normal to a surface. This suggests that, in this condition,  $F(\mathbf{q})$  is particularly sensitive to the displacement of surface atoms in the vertical direction.

Recently, growth simulation of a GaAs(001) surface in homoepitaxy was carried out by using the two-species kinetic growth model on the zinc-blende structure.<sup>23,24</sup> In this simulation, it was revealed that the surface reconstruction is really relevant to the nucleation and growth of homoepitaxial islands on the  $\beta 2(2 \times 4)$ -reconstructed GaAs(001) surface.<sup>23,24</sup> In particular, it was revealed that an island grows by cyclically changing the width of the As dimer rows between 2 and 5 at its edge (see Sec. II and Fig. 3 below).<sup>24</sup> Furthermore, first principles calculations revealed that the displacement of surface atomic coordinates strongly depend

on the details of the reconstruction.<sup>25–27</sup> Thus the scattering of electrons by a terrace edge, even if it occurs, is not so simple as has long been supposed.<sup>7,13,14</sup> In other words, it is not at all clear if the relation  $\Delta I_s \propto -\Delta \rho_e$  really holds on a growing surface.

To study the time evolution of a specular RHEED intensity in the homoepitaxial growth of a GaAs(001) surface on truly atomic scales, we employ the two-species atomistic kinetic growth model.<sup>23,24</sup> By using this model, we calculate the various surface-specific quantities in growth simulations.

This paper is organized as follows. In Sec. I, we critically review simulation studies of GaAs(001) homoepitaxy based on the SOS model and experimental studies based on the STM observations, and point out the incorrectness of the step density model to account for the temporal evolution of a specular RHEED intensity. To show this, we use a more realistic two-species kinetic growth model, which is introduced briefly in Sec. II, and demonstrate the failure of the step density model in Sec. III by explicit kinetic MC simulations. In Sec. IV, we demonstrate the growth simulations, and show evidence that only one of two possible candidates can be relevant to the time evolution of a specular RHEED intensity by examining atomic-scale kinetics both during growth and after interrupting growth. In Sec. V, we carry out *ab initio* calculations on the three different structures appearing in GaAs(001) homoepitaxy, and obtain surface atomic coordinates of these structures to relate our simulation results with a specular RHEED intensity. In view of our results, in Sec. VI we critically discuss whether other studies are viable or not. Section VII is devoted to conclusion.

## II. TWO-SPECIES GROWTH MODEL

To simulate atomic-scale growth kinetics of GaAs(001) homoepitaxy, we use the recently proposed two-species kinetic growth model on the zinc-blende structure.<sup>23,24</sup> In this model, both Ga atoms and As<sub>2</sub> molecules are used as incident species.

By carrying out simulations with this model and comparing the snapshots thus obtained with STM images, it was found that the nucleation of an island having a non-(2 × 4) structure appears on top of the As dimer hill of the  $\beta 2(2 \times 4)$  structure, and that this island grows via the structural transformation to adopt the 2 × 4 structure.<sup>23,24</sup> These processes are seen in the series of the snapshots in Fig. 2, where we can see that the atomic structure fluctuates very strongly when the island is going to adopt the  $\beta 2(2 \times 4)$  structure. By *ab initio* calculations,<sup>28</sup> it was found that the diffusion anisotropy of a Ga adatom is enhanced in the  $[\bar{1}10]$  direction when it is in a trench site of the well-ordered  $\beta 2(2 \times 4)$  structure. However, by simulating growth with the model,<sup>23,24</sup> it was found necessary that this enhancement of the diffusion anisotropy should be turned over to the  $[110]$  direction when a Ga adatom is *not* in a well-ordered trench site of the  $\beta 2(2 \times 4)$  structure.<sup>23,24</sup> Correspondingly, the strong fluctuation found in the transient structures in Fig. 2 is caused by the agreement between the screened Coulomb repulsion between As dimers in the in-plane next-nearest-neighbor sites in the  $[110]$  direction, and the diffusion anisotropy of Ga atoms in the same direction. The importance of this screened Coulomb repulsion for the stability of the

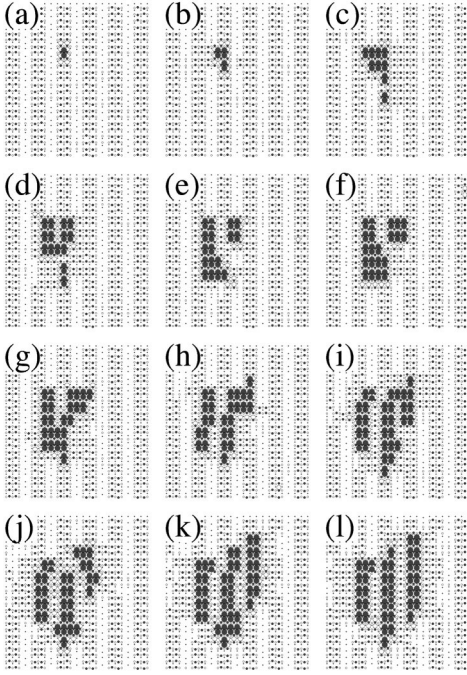


FIG. 2. Simulated process for nucleation and growth of an island to adopt the  $\beta 2(2 \times 4)$  structure. These snapshots were cut out from the  $120a_s \times 120a_s$  lattice. The incident fluxes are  $f_{\text{Ga}} = 0.10$  ML/s and  $f_{\text{As}_2} = 0.40$  ML/s.

$\beta 2(2 \times 4)$  structure was pointed out by Northrup and Froyen.<sup>29</sup> The splitting process of a growing As dimer row is schematically depicted in Fig. 3. When an As dimer suffers from Coulomb repulsion from both right and left sides, as depicted in Figs. 3(d) and 3(e), eventually it will desorb from a surface. Since this process continues at the edge of a growing island, an As dimer row at such an edge changes its width cyclically between 2 and 5, as seen in Fig. 3.

### III. FAILURE OF THE STEP-DENSITY MODEL

As we discussed in Sec. II, when an island grows, the atomic structure at its edge changes ceaselessly by changing the width of an As dimer row there. If this change influences the interaction between an incident electron beam in RHEED observation and surface atoms at the edge of an island, the step-density model becomes very unlikely. To make this point clear, we demonstrate in this section that the time evolution of a step density indeed looks totally different from that of the observed specular RHEED intensities.

In the simulation studies by the one-species SOS model, the step density  $\rho_s$  was defined by counting the number of nearest-neighbor (NN) pairs having different heights as

$$\rho_s = \frac{1}{N} \sum_{\langle \mathbf{x}, \mathbf{x}' \rangle} (1 - \delta_{h(\mathbf{x}), h(\mathbf{x}')}). \quad (1)$$

Here  $h(\mathbf{x})$  denotes the height of a column of atoms, with  $\mathbf{x}$  its two-dimensional (2D) coordinates on the square lattice.  $N$  is the 2D lattice size,  $\delta_{i,j}$  is the Kronecker delta, and the summation runs over all NN pairs.<sup>12–14</sup> Here the azimuthal angle dependence used in Refs. 12 and 13 is not considered, because it is unimportant to our study.

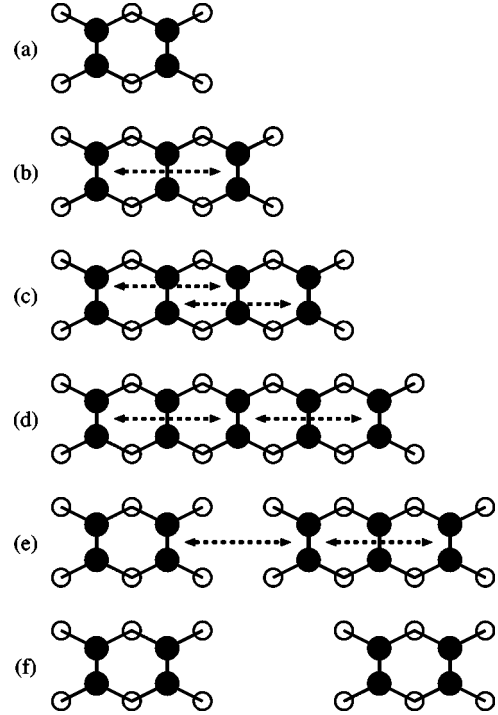


FIG. 3. The splitting process of a growing As dimer row is schematically depicted. The dark and the bright disks denote As and Ga atoms, respectively. The arrows between As dimers in the in-plane next-nearest-neighbor sites denote the screened Coulomb repulsion.

Obviously, this definition can be applied to a one-species system but not to a two-species system, in which heights of both species must be separately specified. This means that we need an alternative definition to Eq. (1), reducing to it after a proper coarse-graining procedure. For this purpose, we first define the presence of an atomic step as follows. Suppose there is a surface atom which lies in the topmost layer. If another topmost-layer atom exists in the in-plane nearest neighborhood, and they both have the same height, then we say that an atomic step does not exist between them. Otherwise, we say that a step exists there. With this definition of an atomic step, which is very general, we consider two different definitions of the step densities. One is the density of NN pairs having heights different from each other, counted irrespective of the surface atomic species, and the other is counted when at least one of the surface atomic species is arsenic.

In Figs. 4(a) and 4(b) we show the results of simulations. These two densities are denoted by  $\rho_a$  and  $\rho_b$ , respectively. They evolve synchronously as functions of time  $t$  in conjunction with the time evolution of the density of Ga adatoms,  $\rho_{\text{Ga}}$ , which is seen in Fig. 4(c).

In the calculations, we use  $f_{\text{Ga}} = 0.10$  and  $f_{\text{As}_2} = 0.40$  monolayers (ML) per second for the fluxes of Ga atoms and  $\text{As}_2$  molecules, respectively. The lattice size is  $120a_s \times 120a_s$ , where the lattice spacing corresponds to  $a_s = 4.0$  Å on a real surface. Growth is started at a time  $t = 0.0$  s, and interrupted at  $t = 20.0$  s.

When growth is started at  $t = 0.0$  s, where no Ga adatoms exist,  $\rho_a(0) = \rho_b(0) = 0.5$ . This is a consequence of the fact that the  $\beta 2(2 \times 4)$  structure consists of double As dimer

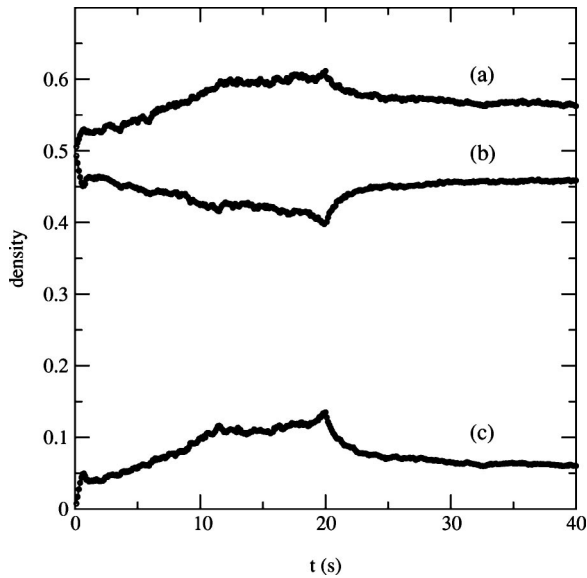


FIG. 4. Step density of a growing GaAs(001) surface derived by calculating the density of steps defined by the NN pairs of surface atoms having different heights counted (a) for all surface atomic pairs irrespective of their species, and (b) when at least one of the surface atomic species is arsenic. For comparison, we show the (c) time evolution of the density of Ga adatoms. The calculation was done on the  $120a_s \times 120a_s$  lattice, and  $f_{\text{Ga}} = 0.10$  ML/s and  $f_{\text{As}_2} = 0.40$  ML/s were used.

rows and double As dimer vacancies. When Ga atoms are deposited, however,  $\rho_a(t)$  increases, while  $\rho_b(t)$  decreases. More precisely, the relations  $\rho_a(t) \approx \rho_a(0) + \rho_{\text{Ga}}(t)$  and  $\rho_b(t) \approx \rho_b(0) - \rho_{\text{Ga}}(t)$  are seen to hold, as naturally expected because Ga adatoms are migrating on an As-terminated surface. Therefore, if surface atomic species are not distinguished,  $\rho_a$  and  $\rho_{\text{Ga}}$  change synchronously as functions of time. If they are distinguished, however, the increase of Ga adatoms results in the decrease of surface As species, and hence,  $\rho_b$  decreases too.

The experimentally observed specular RHEED intensities are seen in Figs. 5(a) and 5(b). Between them, Fig. 5(a) was observed by using  $\text{As}_2$  as the deposition source of arsenic, whereas  $\text{As}_4$  was used in Fig. 5(b). In these figures, the gradual increase of the intensity after several periods of oscillation in each curve is due to the fact that growth was interrupted there.

Since neither of the temporal evolutions of the step densities in Figs. 4(a) and 4(b) resemble the temporal changes of the experimentally observed specular RHEED intensities in Figs. 5(a) or 5(b), the step density model is ruled out as the causal origin of the temporal evolution of a specular RHEED intensity.

#### IV. GROWTH SIMULATION

In Sec. III, we saw the failure of the step density model. We find that there are only two quantities which evolve very similarly to the experimentally observed specular RHEED intensities. Of these two, one is the density of double As dimers  $\rho_{d\text{As}}$ , which is characteristic of the  $\beta 2(2 \times 4)$  structure, and the other is that of the threefold-coordinated Ga atoms supporting As dimers,  $\rho_{\text{Ga}_3}$ . Although  $\rho_{d\text{As}}$  and  $\rho_{\text{Ga}_3}$

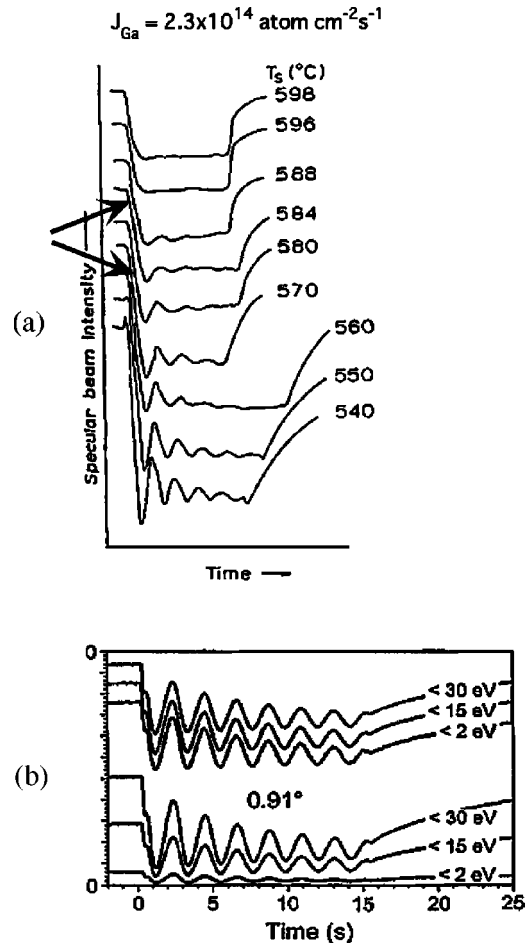


FIG. 5. The experimentally observed specular RHEED intensities (a) with  $\text{As}_2$  (after Ref. 6) and (b) with  $\text{As}_4$  (after Ref. 35). After several periods of oscillations, the intensities increase rather gradually when growth is interrupted.

are identical to each other on the perfectly ordered  $\beta 2(2 \times 4)$  surface, and they even change synchronously, the amplitudes of their temporal variations differ by nearly a factor of 2, as seen in Figs. 6(a) and 6(b). To understand the origin of this difference, suppose that an island is growing on the GaAs(001)- $\beta 2(2 \times 4)$  surface. At the lower side of the edge of an island, the trenches of the  $\beta 2(2 \times 4)$  structure is going to be filled as it grows, and, hence, both  $\rho_{d\text{As}}$  and  $\rho_{\text{Ga}_3}$  decrease by approximately the same amount. On the other hand, threefold-coordinated Ga atoms always exist at the upper side of an edge, where an As dimer row changes its width by growth. Moreover, as an island grows and the width of an As dimer at its edge becomes wider than two,  $\rho_{d\text{As}}$  decreases, while  $\rho_{\text{Ga}_3}$  remains little affected. Thus the oscillation amplitude of  $\rho_{d\text{As}}$  is nearly twice as large as that of  $\rho_{\text{Ga}_3}$ .

The time evolution of  $\rho_{d\text{As}}$  is examined in more detail in Fig. 7(a), which was obtained by the simulations on the  $120a_s \times 120a_s$  lattice.  $f_{\text{Ga}} = 0.10$  ML/s and  $f_{\text{As}_2} = 0.40$  ML/s are used for the incident Ga and  $\text{As}_2$  fluxes. In this figure, we can see that the initial rapid decrease exhibits the transition of the decreasing rate at  $t_A \approx 1.0$  s, which is indicated by the symbol A. The decreasing rate of  $\rho_{d\text{As}}$  is very rapid when  $t < t_A$ , but it becomes a little slower at  $t > t_A$ . This phenomenon occurring at A is more clearly seen

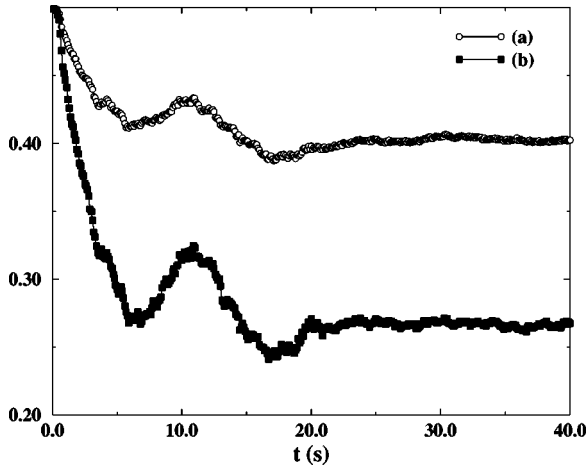


FIG. 6. Time evolutions of (a) the density of threefold-coordinated Ga atoms supporting double As dimers, and (b) the density of double As dimers. The calculation was done on the  $120a_s \times 120a_s$  lattice. The incident fluxes were  $f_{\text{Ga}}=0.10$  ML/s and  $f_{\text{As}_2}=0.40$  ML/s.

in Fig. 8(a), in which the calculation is done on the  $180a_s \times 180a_s$  lattice and the same incident fluxes, i.e.  $f_{\text{Ga}}=0.10$  ML/s and  $f_{\text{As}_2}=0.40$  ML/s are used as before. When these deposition fluxes are reduced to  $f_{\text{Ga}}=0.05$  ML/s and  $f_{\text{As}_2}=0.20$  ML/s, while keeping their ratio fixed, we find that  $t_A$  changes to  $t_A \approx 1.6$  s and not to  $t_A \approx 2.0$  s, as seen in Fig. 8(b). This is because Ga adatoms are allowed to diffuse and reach islands more easily at a lower deposition rate and, hence, the structural transformation is slightly more accelerated in this case.

This transitional behavior is also recognized in the time evolution of the experimentally observed specular RHEED intensities in the temperature range  $570^\circ\text{C} \leq T \leq 588^\circ\text{C}$  in

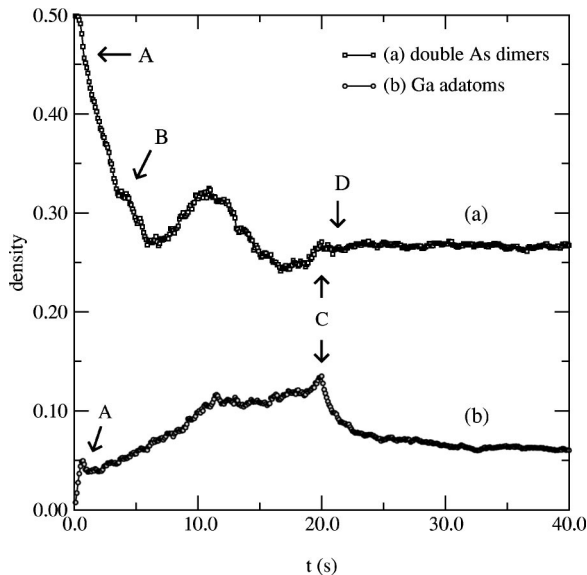


FIG. 7. (a) The time evolution of the density of double As dimers,  $\rho_{d\text{As}}$  calculated on the  $120a_s \times 120a_s$  lattice.  $f_{\text{Ga}}=0.10$  ML/s and  $f_{\text{As}_2}=0.40$  ML/s. The change in the rapid decrease is seen at around  $t_A \approx 1.0$  s, where many initial non- $(2 \times 4)$  islands split to take the  $\beta 2(2 \times 4)$  structure simultaneously. (b) The time evolution of the density of Ga adatoms.

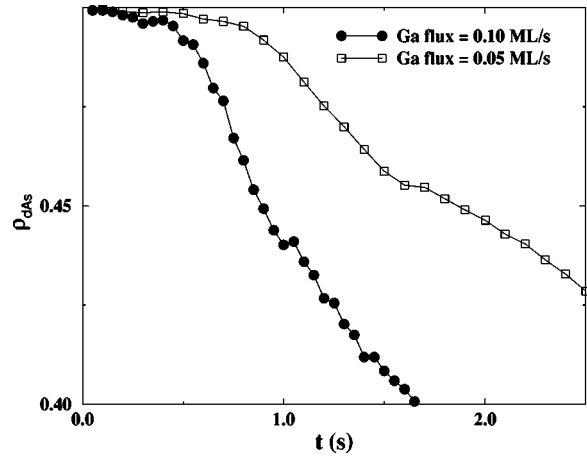


FIG. 8. The time evolution of  $\rho_{d\text{As}}$  at the very early stage of growth, calculated on the  $180a_s \times 180a_s$  lattice. (a)  $f_{\text{Ga}}=0.10$  ML/s and  $f_{\text{As}_2}=0.40$  ML/s.  $t_A \approx 1.0$  s. (b)  $f_{\text{Ga}}=0.05$  ML/s and  $f_{\text{As}_2}=0.20$  ML/s.  $t_A \approx 1.6$  s.

Fig. 5(a), as indicated by arrows for the data obtained at  $T=588$  and  $580^\circ\text{C}$ . This feature is more clearly visible in Fig. 5(b), though they were obtained in the experiments by using  $\text{As}_4$  instead of  $\text{As}_2$  for the arsenic flux in MBE growth. According to our simulation results, this change in the decreasing rate of the specular RHEED intensity results from the fact that when small islands appear on top of the well-ordered  $\beta 2(2 \times 4)$  substrate, they grow and tend to have As dimer rows with widths wider than 3; then many of them split and adopt the  $\beta 2(2 \times 4)$  structure almost simultaneously.<sup>23,24</sup> This is because the barrier for the rate-limiting process of this splitting phenomenon is very large, i.e., it is the barrier for the desorption of the As dimer in the central site, denoted in gray in Fig. 9(a) with a value as large as 2.22 eV, followed by the desorption of other As dimers in the same row, denoted in gray in Fig. 9(b) with a barrier of 1.88 eV. Hence, the splitting process proceeds rather slowly on many islands almost simultaneously, to become macroscopically detectable by RHEED observation. In accordance with the evolution of this surface morphology, the density of Ga adatoms  $\rho_{\text{Ga}}$  evolves, as seen in Fig. 7(b), showing that

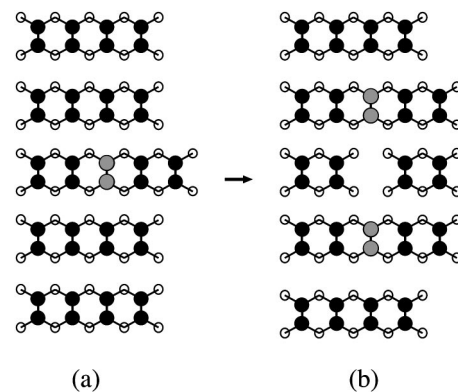


FIG. 9. (a) The desorption of an As dimer in the central site of the five-wide dimer row. The desorption barrier of the gray As dimer is 2.22 eV. (b) The splitting process that follows the desorption depicted in (a). The desorption barrier of the gray As dimers is 1.88 eV.

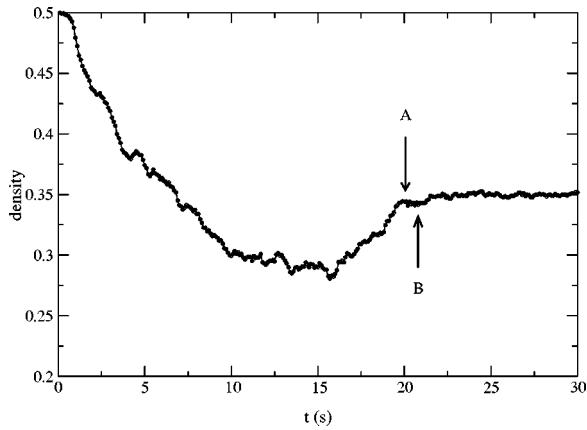


FIG. 10. The time evolution of  $\rho_{dAs}$  for growth interrupted at  $\theta=1.0$  ML. The Ga flux is 0.05 ML/s and the  $As_2$  flux is 0.20 ML/s. The lattice size is  $180a_s \times 180a_s$ . The growth is interrupted at A, and the density of double As dimers reaches the minimum at B.

the initial linear increase of this density stops at  $t \approx 0.5$  s due to the nucleation of islands, and it begins to decrease until time  $t$  reaches  $t_A$ , where the structural change of the islands takes place. Then it increases again till  $t \approx 12.0$  s after a short period of a plateau at  $1.0 \leq t \leq 2.0$  s. The appearance of this short plateau shows that the structural transformation to adopt the  $\beta 2(2 \times 4)$  structure, and the growth of small islands immediately afterward, which we saw in Fig. 2, are actually very efficient in incorporating Ga adatoms, whereas the nearly constant increase of  $\rho_{Ga}$  at  $2.0 \leq t \leq 12.0$  s indicates that growth of islands having the  $\beta 2(2 \times 4)$  structure is rather inefficient in this process.

In Fig. 7(a), there is a fluctuation in  $\rho_{dAs}$  at around  $t \approx 4$  s indicated by the symbol B. This is simply caused by the coalescence of islands, which appears so prominently because each coalescence phenomenon significantly affects the density of double As dimers when the system size is rather small. Therefore, this is a finite-size effect, which becomes negligible when the system size is made larger. This is because coalescence occurs at several different sites independently of each other. In deep contrast to this, the amplitude of the fluctuation associated with the structural transformation at  $t \approx t_A$  is independent of the system size because the structural change proceeds on many different islands almost simultaneously.

In contrast to the fluctuation at B, the fast decrease of  $\rho_{dAs}$  at D has a physical significance. Actually, when the deposition of Ga atoms is interrupted at C, diffusive Ga adatoms are quickly incorporated into the edges of the pre-existing islands, and transform the local structure from the  $\beta 2(2 \times 4)$  structure to the  $\beta 1(2 \times 4)$  structure, or even wider As dimer row structures. Then, since the deposition of Ga atoms is already interrupted, there are not so many Ga atoms available to enable the quick splitting of wide As dimer rows so as to change it back to the  $\beta 2(2 \times 4)$  structure. Therefore, these As dimer rows stay wide for a substantially long period of time, until phase ordering causes them to transform back into the  $\beta 2(2 \times 4)$  structure.

This process is also seen in Fig. 10, which was obtained with the fluxes of  $f_{Ga}=0.05$  ML/s and  $f_{As_2}=0.20$  ML/s, and a lattice size of  $180a_s \times 180a_s$ . In this calculation, to

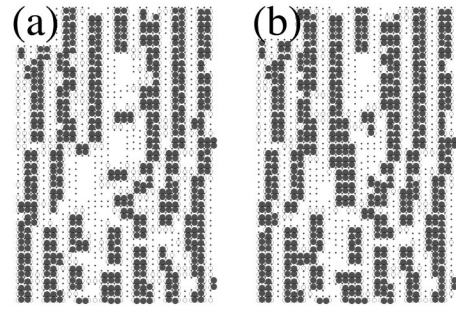


FIG. 11. A pair of the snapshots showing the morphology change immediately after interrupting growth. (a) and (b) correspond to A and B in Fig. 10, respectively.

avoid any multilayer effects, growth was interrupted at A, i.e.,  $t=20.0$  s, where the coverage reached  $\theta=1.0$  ML. Here, the coverage  $\theta$  is defined by  $\theta=tf_{Ga}$ . After the interruption of growth at A,  $\rho_{dAs}$  decreased until it reached the minimum value at B. The snapshots at A and B are seen in Figs. 11(a) and 11(b), which were cut out from the  $180a_s \times 180a_s$  lattice, to show the change between A and B. In Fig. 11(b), we see the appearance of several wide As dimer rows at the central region. In RHEED experiments, this decrease is recognized in many of the specular RHEED intensity data in Ref. 13. At the same time, however, this feature is less prominent in Fig. 6(a). These results suggest that, when the diffraction condition of a specular RHEED intensity on GaAs(001) is adjusted to observe the  $\beta 2(2 \times 4)$  structure, double As dimer rows are relevant to the specular RHEED intensity.

Though Figs. 6(a) and 6(b) do not show sufficiently large recoveries after interrupting growth at  $t=20.0$  s, this is due to the fact that the rigid lattice model we used does not admit local deformations of surface atomic coordinates off lattice sites, so that coalescence, in which a cooperative deformation of the coordinates of many surface atoms are presumably involved, cannot proceed quickly. Instead, these results as well as Figs. 7(a) and 7(b) imply the origin of the experimentally observed fast and slow recoveries of a specular RHEED intensity after interrupting growth.<sup>5</sup> That is, Figs. 7(a) and 7(b) indicate that the fast recovery is due to the incorporation of Ga adatoms into existing islands or to step edges surrounding voids to fill them in, and the slow recovery is due to the phase ordering during coalescence of various islands consisting of the  $\beta 2(2 \times 4)$  structure.<sup>5</sup> Indeed, if the fast decrease of  $\rho_{Ga}$  in Fig. 7(b) is characterized by the exponential form  $-\exp(-t/\tau)$ , we obtain the characteristic time  $\tau \approx 2.5$  s for the interval  $20.0 \leq t \leq 22.0$  s. This value is very close to  $\tau_1 \approx 2.3 \pm 0.2$  s, which was obtained for the fast recovery process of RHEED intensity observation.<sup>5</sup> Therefore, our simulations account for the principal features of a specular RHEED intensity both during and after interrupting growth.

In our model calculations, the density of Ga adatoms reaches about 10–15% of the surface area when the coverage  $\theta$  ranges  $\theta=1-2$  ML, as seen in Fig. 7(b). Most of these adatoms are migrating in trenches during growth by locally taking an  $\alpha(2 \times 4)$  structure. Therefore, this is in rough agreement with Morris *et al.*'s theoretical analyses<sup>30</sup> of the reflection anisotropy spectroscopy (RAS)

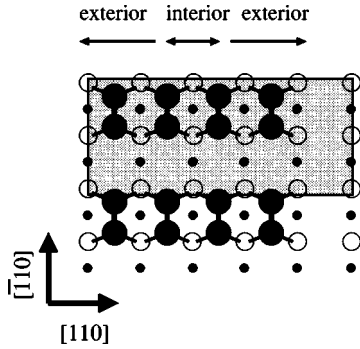


FIG. 12. Plan views of the  $2 \times 5$  structure. The hypothetical unit cell and the crystallographic directions are indicated by the shaded rectangle and the arrows, respectively. The dark and bright disks denote As and Ga atoms, respectively, and their radii decrease according to their depths. The distinction between the interior and exterior As dimers is used in Table I.

measurement,<sup>31</sup> in which about 20% of the *as-grown* surface was found to consist of the  $\alpha(2 \times 4)$  structure<sup>32</sup> to indicate the high population of Ga adatoms during growth.<sup>33</sup> This further accounts for the fact that, when growth is interrupted, a specular RHEED intensity on a real GaAs(001) surface decreases more prominently than those we obtained by simulations, as seen in Figs. 7(a) and 10, because the amount of surplus Ga adatoms can be larger on a real surface than in the simulations.

Our results suggest that the density of double As dimers is relevant to a specular RHEED intensity when it is observed with the growth condition adjusted to realize exclusively the  $\beta 2(2 \times 4)$  structure. Thus it is shown that a surface reconstruction is really relevant to a specular RHEED intensity. In Sec. V, we compare our results with those obtained by *ab initio* calculations, and relate our simulation results to experimental observations.

## V. AB INITIO CALCULATIONS

In Sec. IV, we showed several convincing results to evidence the relevance of the density of double As dimers to the occurrence of electron diffraction in specular RHEED observation. In order to further confirm this, we need to know in detail how surface atomic structures deform during growth. To this aim, we carry out *ab initio* energy-minimization calculations on three different structures—i.e., the  $\beta 2(2 \times 4)$  structure, the  $\beta 1(2 \times 4)$  structure, and the  $2 \times 5$  structure—by fixing the coordinates of the seventh-layer As atoms.<sup>34</sup> The details of the calculation method was described elsewhere.<sup>25</sup> Among these three structures, the first two structures are seen in Figs. 1(a) and 1(b), respectively, whereas the last one is depicted in Fig. 12. Despite that the metastable structures such as the quadruple As dimer row in Fig. 3(c) always appears in kinetic MC simulations as aperiodic structures, we carry out calculations by assuming the periodicity of these structures. These results of the *ab initio* calculations are compiled in Tables I and II. In Table I,  $d$  and  $w$  denote the bond lengths of the As dimers and their spacing in the  $[110]$  direction, respectively, while  $\Delta h_{As-As}$  denotes the height difference between the As atoms in the first and seventh layers. Those seen in Table II are the height differ-

TABLE I. The results of *ab initio* calculations on the deformation of surface atoms for the  $\beta 2(2 \times 4)$  structure, the  $\beta 1(2 \times 4)$  structure, and the  $2 \times 5$  structure. The dimer bond length and dimer spacing of the first layer As dimers are denoted by  $d$  and  $w$ , respectively. The height difference between the As atoms in the first and seventh layers is denoted by  $\Delta h_{As-As}$ . For the definitions of the interior and exterior As dimers, see Fig. 12. The similar distinction of the As dimers is also applied to the  $\beta 1(2 \times 4)$  structure in Fig. 1(b).

Structure	As dimer	$d$ (Å)	$w$ (Å)	$\Delta h_{As-As}$ (Å)
$\beta 2(2 \times 4)$		2.51	3.81	8.22
$\beta 1(2 \times 4)$	interior	2.50	3.83	8.22
	exterior	2.51		8.25
$2 \times 5$	interior	2.45	3.96	8.14
	exterior	2.52	3.86	8.28

ences between the second-layer Ga atoms and the seventh-layer As atoms. In this table, the leftmost entities are those of the interior sites, and those in the exterior sites are displayed on the right side if they exist. As the second-layer Ga atoms at the outer edge of these structures tend to adopt  $sp^2$ -rehybridized orbitals, they are inclined toward the interior of the As dimer block, and push As dimers on top of them slightly upwards. Due to this, in particular, As dimers at the exterior sites of both  $\beta 1(2 \times 4)$  structure and  $2 \times 5$  structures have larger heights than those in the interior sites of these structures [see Figs. 1(a), 1(b), and 12]. However, there is a clear difference in the displacement of the interior As dimers between these structures. That is, as exterior As dimers move upward, the interior one in the  $\beta 1(2 \times 4)$  structure moves somewhat upward as well. In contrast, the interior As dimers in the  $2 \times 5$  structure do not move upwards in association with the displacement of the exterior ones. In both cases, however, the height differences between the interior and exterior ones are significantly large when they are compared with  $\lambda$  ( $< 0.13$  Å). Contrary to these differences in the atomic coordinates of the As dimers among these three structures, the heights of the second-layer Ga atoms change moderately in a monotonic manner from interior sites to exterior sites, as seen in Table II.

We note that although these results were obtained by assuming the periodicity of metastable  $\beta 1(2 \times 4)$  and  $(2 \times 5)$  structures, our results suggest that these structures do not satisfy the diffraction condition of an incident electron beam used in RHEED observation when it is adjusted to observe the  $\beta 2(2 \times 4)$  structure.

TABLE II. The height differences between the second-layer Ga atoms and the seventh-layer As atoms are displayed in order from the interior site to the exterior site. The second column is used for the Ga atoms in the exterior sites of the  $2 \times 4$  structures or those in the middle sites of the  $2 \times 5$  structure. The third column is used for the Ga atoms in the exterior sites of the  $2 \times 5$  structure.

Structure	interior (Å)	second (Å)	third (Å)
$\beta 2(2 \times 4)$	6.75	6.49	
$\beta 1(2 \times 4)$	6.78	6.55	
$2 \times 5$	6.83	6.79	6.58

## VI. DISCUSSION

In this section, we discuss the physical significance of our results by comparing them with those obtained by other studies. In particular, we discuss whether other theoretical as well as experimental results are still viable or not.

By the kinetic MC simulations of GaAs(001) homoepitaxy, we find that the time evolution of a specular RHEED intensity cannot be accounted for by using the density of atomic steps. Instead, we find that a specular RHEED intensity and the density of double As dimers evolve synchronously. Comparison of the results between these kinetic MC simulation and *ab initio* calculations suggests that our results are valid when the diffraction condition of a specular RHEED intensity is initially set to observe the  $\beta 2(2 \times 4)$  structure.

In general, multiple-scattering effects make a finite contribution to a specular RHEED intensity. Even if such a process is involved, the leading-order contribution to the time evolution of a specular RHEED intensity must be linear in the time evolution of surface atomic structures, and all other effects can have only subleading contributions to it. Therefore, our results provide evidence that the temporal evolution of surface atomic structures is indeed relevant to the time evolution of a specular RHEED intensity. These results are consistent with the experimental results obtained by Braun and co-workers,<sup>35,36,11</sup> who demonstrated that the phase shift of the observed specular RHEED intensity oscillations can be well accounted for by taking account of the fact that the reconstructed surface layer has a different thickness than that in the bulk structure. The relevance of this thickness difference to experimental observations of the specular RHEED intensities was pointed out by Horio and Ichimiya,<sup>37,38</sup> for the first time. The importance of the relaxation of surface structure was also pointed out by McCoy *et al.* to achieve good agreement between the dynamical RHEED calculations and experimental data.<sup>39</sup>

In another theoretical dynamical diffraction study,<sup>40</sup> while it is stated that the geometry of the GaAs(001)- $\beta 2(2 \times 4)$  structure was assumed, deformation of surface atoms was not considered. However, since this deformation constitutes a very important part of the reconstruction, this treatment is obviously inconsistent.

In order to realize a slow recovery process after interrupting growth, a step-edge barrier was introduced into the SOS model so as to hinder a surface from flattening.<sup>41</sup> However, this cannot be correct because the SOS model does not possess an atomic scale accuracy, so that its lower bound on the range of the applicability is much larger than  $a_s = 4.0 \text{ \AA}$  when applied to a GaAs(001) surface, while the introduction of a step-edge barrier requires the model to possess an atomic scale accuracy. Therefore, it is inconsistent to introduce a step-edge barrier into the SOS model for the purpose of studying growth on a GaAs(001) surface or on an InAs(001) surface.<sup>16,41,42</sup> In contrast, Heyn and co-workers considered a two-species extension of the SOS model,<sup>43,44</sup> and derived the conclusion that the fast recovery process is due to Ga species, whereas both species are involved in the slow recovery process. Thus, our results and theirs are consistent with each other.

For the nucleation mechanism of islands in GaAs(001)

homoepitaxy, Kratzer *et al.* recently proposed, based entirely on *ab initio* energy-minimization calculations,<sup>45</sup> another scenario than what we demonstrated in Sec. II. In their calculations, they first supplied Ga atoms onto the  $\beta 2(2 \times 4)$  substrate in the absence of As flux to let them settle down to preferential sites, i.e., trench sites; later, they supplied As<sub>2</sub> dimers onto this structure. With these results, they concluded that the nucleation of islands takes place by at first filling in trench sites with Ga as well as As species to change the surface structure from the  $\beta 2(2 \times 4)$  structure to the  $\beta 1(2 \times 4)$  structure. According to their scenario, which is actually the same as that proposed by Shiraishi and Ito several years ago,<sup>46–49</sup> a considerable portion of a GaAs(001) surface must change from a  $\beta 2(2 \times 4)$  structure to a  $\beta 1(2 \times 4)$  structure soon after starting growth. On the other hand, the STM images obtained immediately after starting growth shows the stability of the  $\beta 2(2 \times 4)$  structure even near the growing islands.<sup>23,50</sup> Moreover, the surface structure observed by STM was confirmed repeatedly by several groups to consist of the  $\beta 2(2 \times 4)$  structure.<sup>20–22,51</sup> Therefore, this alternative scenario does not correspond to the homoepitaxial growth of a GaAs(001)- $(2 \times 4)$  surface realized in the usual MBE growth conditions, in which, unlike the *ab initio* calculation studies in Refs. 45–49, both Ga and As species are supplied simultaneously onto a substrate surface at  $T > 500 \text{ }^\circ\text{C}$ . Instead, the growth condition used in the scenario proposed by Shiraishi and Ito and Kratzer *et al.* is much closer to that of migration-enhanced epitaxy<sup>52</sup> rather than to usual MBE. In general, the structure of an MBE-grown GaAs(001) surface strongly depends on the substrate temperature and the III-V flux ratio used in growth,<sup>8,22,50,53–55</sup> and the *ab initio* calculations in Refs. 9 and 10 also suggest this dependence, but the *ab initio*-based growth studies in Refs. 45–49 do not capture these important properties.

For clarity, we show how a positive correlation appears in the time evolutions between  $I_s$  and  $\bar{\rho}_e = 1 - \rho_e$ . To this end, we denote the time evolving part of  $I_s$  by  $I_s^{(t)}$ . On a growing surface, suppose that there are various islands, or more generally, domains, labeled by  $i (i = 1, 2, \dots)$ , which consist of particular surface structures labeled by  $\alpha_i$ . Suppose further that each domain has an area with its density denoted by  $\rho_i(\alpha_i)$ , and its efficiency of electron diffraction is represented by a coefficient  $c(\alpha)$ . With the use of these, our results suggest that the principal contribution to  $I_s^{(t)}$  comes from the atomic structures of a growing surface, so that  $I_s^{(t)}$  is approximately given by  $I_s^{(t)} \simeq \sum_i c(\alpha_i) \rho_i(\alpha_i)$ . On the other hand, if we denote the density of surface defects such as point defects or phase boundaries by  $\rho_d$ , the summation of all densities amounts to unity,  $\sum_i \rho_i(\alpha_i) + \rho_e + \rho_d = 1$ . Therefore, when a particular surface structure  $\alpha_0$  is uniquely selected by an appropriate growth condition,  $I_s^{(t)}$  reduces to  $I_s^{(t)} \simeq c(\alpha_0) \sum_i \rho_i(\alpha_0) = c(\alpha_0)(1 - \rho_e - \rho_d)$ , which further reduces to  $I_s^{(t)} \simeq c(\alpha_0)(1 - \rho_e) = c(\alpha_0)\bar{\rho}_e$  only when  $\rho_e \gg \rho_d$ . Thus  $I_s^{(t)}$  and  $\bar{\rho}_e$  change synchronously only when the growth condition is chosen to realize a particular surface reconstruction uniquely so as to avoid a structural degeneracy, and also when the densities of phase boundaries and other surface defects are negligibly small.<sup>15–17</sup> However, since we saw in Fig. 4 that step densities with two different definitions did not oscillate during growth, this latter condition does not



necessary hold on a growing surface at high temperature. Therefore, in order to reinterpret properly the STM images in Refs. 15–17, which were obtained by quenching the sample surfaces down to room temperature after interrupting growth, we must take account of the facts that (1) the density of Ga adatoms rapidly decreases after interrupting growth, i.e., after terminating Ga deposition, as seen in Fig. 7(b); and (2) in general, stable structures are more favored as the temperature is decreased. Based on these assumptions, we conclude that the rather good agreement in the time evolutions between  $I_s^{(t)}$  and  $\bar{\rho}_e$  obtained in Refs. 15–17 resulted because the process of quenching after interrupting growth causes metastable structures to transform into stable structures, so that the inequality  $\rho_e \gg \rho_d$  is enforced by these post-growth treatments. In particular, since our result in Fig. 6(b) shows that the density of Ga adatoms reaches as high as 15% at  $t \approx 20.0$  s, or equivalently, at  $\theta \approx 2.0$  ML, it is certainly possible that these atoms are incorporated into the surface structure, and locally rearrange them to decrease  $\rho_d$  significantly during a quenching process.

In contrast, when a surface has a structural degeneracy, these two *macroscopic* quantities generally do not correlate with each other. One example is the growth of the Ge(111) surface, on which the specular RHEED intensity does not exhibit a simple sinusoidal oscillation with a gradually decreasing amplitude at low temperatures. Instead, it shows a double-periodic oscillation.<sup>56</sup> Another example is the reentrant layer-by-layer growth of a GaAs(111) surface, on which the RHEED observation revealed the phase difference between the oscillations at high-temperature Ga vacancy reconstruction and those at low-temperature As trimer reconstruction.<sup>57</sup> As is clear from our argument, these phenomena are well accounted for by the structural change in the surface reconstructions,<sup>58</sup> and not by step densities.<sup>59</sup> The significant difference in the amplitude of the RHEED intensities between these two structures on GaAs(111) (Ref. 57) indicates that the displacement of surface atoms plays an important role in electron diffraction.

Then we must ask why the step-density model, combined with the SOS model, agreed well with the specular RHEED intensities observed on Si(001).<sup>12</sup> In Refs. 12–14, comparisons were made between  $I_s^{(t)}$  and  $\bar{\rho}_s = 1 - \rho_s$ , with  $\rho_s$  given in Eq. (1). Thus, in fact,  $\bar{\rho}_s = (1/N) \sum_{\langle \mathbf{x}, \mathbf{x}' \rangle} \delta_{h(\mathbf{x}), h(\mathbf{x}')} + \text{const}$ , i.e.,  $\bar{\rho}_s$  actually calculates the density of ordered areas, in

which the possible appearance of phase boundaries as well as other surface defects is thoroughly neglected by the crude simplification of the SOS model.<sup>60</sup> Since dimer reconstruction on Si(001) and Ge(001) is associated with atomic displacement,<sup>61</sup> an argument similar to that given in the present study can also certainly be applied to these surfaces.

## VII. CONCLUSION

By kinetic MC simulations, we found that the density of double As dimers on a surface evolves synchronously with the observed time evolutions of specular RHEED intensities in the homoepitaxial growth of a GaAs(001)- $\beta 2(2 \times 4)$  surface. The results of our *ab initio* calculations suggest that they evolve similarly when the diffraction condition is set to observe the  $\beta 2(2 \times 4)$  structure. They also suggest that it is crucial that surface atoms in the transient structures be displaced differently from those in the  $\beta 2(2 \times 4)$  structure. Furthermore, we found that the fast and slow recoveries of a specular RHEED intensity after interrupting growth are due to the incorporation of Ga adatoms and the phase ordering of the  $\beta 2(2 \times 4)$  structure, respectively. In addition, we found that the density of atomic steps does not oscillate during growth, so that it does not have any relations to the time evolution of a specular RHEED intensity. Instead, the virtually positive correlation between them appears only after taking the average of the densities of surface reconstructions over a large area on a quenched surface.

## ACKNOWLEDGMENTS

Dr. J. H. Neave and Dr. G. R. Bell are greatly acknowledged for their collaborations at the initial stage of this work, Dr. W. Braun for his correspondence, Professor A. Ichimiya for his fruitful discussions on dynamical RHEED calculations, and Professor T. Nakayama for his discussions and correspondence on RAS. This work was initiated when one of the authors (M.I.) was at Imperial College London, with the financial support by Engineering and Physical Sciences Research Council of the United Kingdom. He would like to express his sincere thanks to Professor G. Parry, Professor C. Isham, Professor M. Blencowe, Professor K. L. Vodopyanov, Dr. M. Chu, and Dr. E. Hofstetter for their encouragement.

\*Present address: Department of Physics, Graduate School of Science, Osaka University, Toyonaka, Osaka 560-0043, Japan. Electronic address: makoto@acty.phys.sci.osaka-u.ac.jp

<sup>1</sup>*Molecular Beam Epitaxy*, edited by Alfred Cho (AIP, New York, 1994).

<sup>2</sup>J.J. Harris, B.A. Joyce, and P.J. Dobson, *Surf. Sci.* **103**, L90 (1981).

<sup>3</sup>C.E.C. Wood, *Surf. Sci.* **108**, L441 (1981).

<sup>4</sup>J.M. Van Hove, C.S. Lent, P.R. Pukite, and P.I. Cohen, *J. Vac. Sci. Technol. B* **1**, 741 (1983).

<sup>5</sup>J.H. Neave, B.A. Joyce, P.J. Dobson, and N. Norton, *Appl. Phys. A: Solids Surf.* **31**, 1 (1983).

<sup>6</sup>J.H. Neave, P.J. Dobson, B.A. Joyce, and J. Zhang, *Appl. Phys. Lett.* **47**, 100 (1985).

<sup>7</sup>J. Zhang, J.H. Neave, B.A. Joyce, P.J. Dobson, and P.N. Fawcett, *Surf. Sci.* **231**, 379 (1990).

<sup>8</sup>For reviews on the GaAs(001)- $2 \times 4$  structures, see C.M. Goringe, L.J. Clark, M.H. Lee, M.C. Payne, I. Štich, J.A. White, M.J. Gillan, and A.P. Sutton, *J. Phys. Chem.* **101**, 1498 (1997); Q.-K. Xue, T. Hashizume, and T. Sakurai, *Prog. Surf. Sci.* **56**, 1 (1997).

<sup>9</sup>J.E. Northrup and S. Froyen, *Phys. Rev. Lett.* **71**, 2276 (1993).

<sup>10</sup>N. Moll, A. Kley, E. Pehlke, and M. Scheffler, *Phys. Rev. B* **54**, 8844 (1996).

<sup>11</sup>W. Braun, *Applied RHEED* (Springer-Verlag, Berlin, 1999).

<sup>12</sup>S. Clarke and D.D. Vvedensky, *Phys. Rev. Lett.* **58**, 2235 (1987); *Phys. Rev. B* **36**, 9312 (1987); *Surf. Sci.* **189**, 1033 (1987); *J. Appl. Phys.* **63**, 2272 (1988); *Phys. Rev. B* **37**, 6559 (1988).

- <sup>13</sup>T. Shitara, D.D. Vvedensky, M.R. Wilby, J. Zhang, J.H. Neave, and B.A. Joyce, *Phys. Rev. B* **46**, 6815 (1992).
- <sup>14</sup>T. Shitara, D.D. Vvedensky, M.R. Wilby, J. Zhang, J.H. Neave, and B.A. Joyce, *Phys. Rev. B* **46**, 6825 (1992).
- <sup>15</sup>J. Sudijono, M.D. Johnson, C.W. Snyder, M.B. Elowitz, and B.G. Orr, *Phys. Rev. Lett.* **69**, 2811 (1992).
- <sup>16</sup>M.D. Johnson, C. Orme, A.W. Hunt, D. Graff, J. Sudijono, L.M. Sander, and B.G. Orr, *Phys. Rev. Lett.* **72**, 116 (1994).
- <sup>17</sup>D.M. Holmes, J.L. Sudijono, C.F. McConville, T.S. Jones, and B.A. Joyce, *Surf. Sci.* **370**, L173 (1997).
- <sup>18</sup>Y.W. Mo, J. Kleiner, M.B. Webb, and M.G. Lagally, *Phys. Rev. Lett.* **66**, 1998 (1991).
- <sup>19</sup>Y.W. Mo, J. Kleiner, M.B. Webb, and M.G. Lagally, *Surf. Sci.* **268**, 275 (1992).
- <sup>20</sup>T. Hashizume, Q.-K. Xue, J. Zhou, A. Ichimiya, and T. Sakurai, *Phys. Rev. Lett.* **73**, 2208 (1994).
- <sup>21</sup>T. Hashizume, Q.-K. Xue, A. Ichimiya, and T. Sakurai, *Phys. Rev. B* **51**, 4200 (1995).
- <sup>22</sup>A.R. Avery, C.M. Goringe, D.M. Holmes, J.L. Sudijono, and T.S. Jones, *Phys. Rev. Lett.* **76**, 3344 (1996).
- <sup>23</sup>M. Itoh, G.R. Bell, A.R. Avery, T.S. Jones, B.A. Joyce, and D.D. Vvedensky, *Phys. Rev. Lett.* **81**, 633 (1998).
- <sup>24</sup>M. Itoh, Ph.D. thesis, University of London 1999, which is available at <http://www.wacty.phys.sci.osaka-u.ac.jp/~makoto/>
- <sup>25</sup>T. Ohno, *Phys. Rev. Lett.* **70**, 631 (1993).
- <sup>26</sup>G.P. Srivastava and S.J. Jenkins, *Phys. Rev. B* **53**, 12 589 (1996).
- <sup>27</sup>G.P. Srivastava and S.J. Jenkins, *Surf. Rev. Lett.* **5**, 219 (1998).
- <sup>28</sup>A. Kley, P. Ruggerone, and M. Scheffler, *Phys. Rev. Lett.* **79**, 5278 (1997).
- <sup>29</sup>J.E. Northrup and S. Froyen, *Phys. Rev. B* **50**, 2015 (1994).
- <sup>30</sup>S.J. Morris, J.M. Bass, and C.C. Matthai, *Phys. Rev. B* **52**, 16 739 (1995).
- <sup>31</sup>I. Kamiya, D.E. Aspnes, L.T. Florez, and J.P. Harbison, *Phys. Rev. B* **46**, 15 894 (1992).
- <sup>32</sup>It is not clear if the mixing ratio between two structures on a high-temperature growing surface can be uniquely determined by comparing the calculated and observed RAS data in the manner Morris *et al.* claimed in Ref. 30. See also M. Murayama, K. Shiraishi, and T. Nakayama, *Jpn. J. Appl. Phys., Part 1* **37**, 4109 (1998).
- <sup>33</sup>J. Tersoff, M.D. Johnson, and B.G. Orr, *Phys. Rev. Lett.* **78**, 282 (1997).
- <sup>34</sup>Our results on the atomic coordinates of the  $\beta 2(2 \times 4)$  structure are slightly different from those reported in Refs. 26 and 27 with regard to the deformation of As dimers.
- <sup>35</sup>W. Braun, L. Däweritz, and K.H. Ploog, *Phys. Rev. Lett.* **80**, 4935 (1998).
- <sup>36</sup>W. Braun, L. Däweritz, and K.H. Ploog, *J. Vac. Sci. Technol. B* **16**, 2404 (1998).
- <sup>37</sup>Y. Horio and A. Ichimiya, *Surf. Sci.* **298**, 261 (1993).
- <sup>38</sup>Y. Horio and A. Ichimiya, *Jpn. J. Appl. Phys., Part 2* **33**, L377 (1994).
- <sup>39</sup>J.M. McCoy, U. Korte, and P.A. Maksym, *Surf. Sci.* **418**, 273 (1998).
- <sup>40</sup>Z. Mitura, S.L. Dudarev, and M.J. Whelan, *Phys. Rev. B* **57**, 6309 (1998).
- <sup>41</sup>P. Šmilauer and D.D. Vvedensky, *Phys. Rev. B* **48**, 17 603 (1993).
- <sup>42</sup>M.F. Gyure, J.J. Zinck, C. Ratsch, and D.D. Vvedensky, *Phys. Rev. Lett.* **81**, 4931 (1998).
- <sup>43</sup>Ch. Heyn and M. Harsdorff, *Phys. Rev. B* **55**, 7034 (1997).
- <sup>44</sup>Ch. Heyn, T. Franke, R. Anton, and M. Harsdorff, *Phys. Rev. B* **56**, 13 483 (1997).
- <sup>45</sup>P. Kratzer, C.G. Morgan, and M. Scheffler, *Phys. Rev. B* **59**, 15 246 (1999).
- <sup>46</sup>K. Shiraishi and T. Ito, *Surf. Sci.* **358**, 451 (1996).
- <sup>47</sup>K. Shiraishi and T. Ito, *Surf. Sci.* **386**, 241 (1997).
- <sup>48</sup>T. Ito and K. Shiraishi, *Jpn. J. Appl. Phys., Part 1* **37**, 4234 (1998).
- <sup>49</sup>T. Ito and K. Shiraishi, *Appl. Surf. Sci.* **121**, 171 (1997).
- <sup>50</sup>K. Kanisawa and H. Yamaguchi, *Phys. Rev. B* **56**, 12 080 (1997).
- <sup>51</sup>V.P. LaBella, H. Yang, D.W. Bullock, P.M. Thibado, P. Kratzer, and M. Scheffler, *Phys. Rev. Lett.* **83**, 2989 (1999).
- <sup>52</sup>Y. Horikoshi, *Semicond. Sci. Technol.* **8**, 1032 (1993), and references therein.
- <sup>53</sup>A.R. Avery, D.M. Holmes, J.L. Sudijono, T.S. Jones, and B.A. Joyce, *Surf. Sci.* **323**, 91 (1995).
- <sup>54</sup>G.R. Bell, J.G. Belk, C.F. McConville, and T.S. Jones, *Phys. Rev. B* **59**, 2947 (1999).
- <sup>55</sup>D.K. Biegelsen, R.D. Bringans, J.E. Northrup, and L.E. Swartz, *Phys. Rev. B* **41**, 5701 (1990).
- <sup>56</sup>K. Fukutani, H. Daimon, and S. Ino, *Jpn. J. Appl. Phys., Part 1* **31**, 3429 (1992).
- <sup>57</sup>P.H. Steans, J.H. Neave, E.S. Tok, G.R. Bell, B.A. Joyce, and T.S. Jones, *J. Cryst. Growth* **201-202**, 198 (1999).
- <sup>58</sup>M. Itoh, *Phys. Rev. B* **58**, 6716 (1998).
- <sup>59</sup>T. Yokotsuka, M.R. Wilby, D.D. Vvedensky, T. Kawamura, K. Fukutani, and S. Ino, *J. Cryst. Growth* **127**, 479 (1993); *Appl. Phys. Lett.* **62**, 1673 (1993).
- <sup>60</sup>B. Voigtländer, T. Weber, P. Šmilauer, and D.E. Wolf, *Phys. Rev. Lett.* **78**, 2164 (1997).
- <sup>61</sup>M. Needels, M.C. Payne, and J.D. Joannopoulos, *Phys. Rev. Lett.* **58**, 1765 (1987).